

Internal Waves and Synchronized Precession in a Cold Vapor

M. Ö. Oktel¹ and L. S. Levitov²

¹*Department of Physics, The Ohio State University, 174 West 18th Avenue, Columbus, Ohio 43210*

²*Department of Physics, Massachusetts Institute of Technology, 77 Massachusetts Avenue, Cambridge, Massachusetts 02139*

(Received 26 November 2001; published 23 May 2002)

Exchange in a Boltzmann gas of bosons with several internal states leads to collective transport of internal polarization. The internal dynamics can be understood as Larmor precession in the presence of a torque induced by atoms on each other via exchange coupling. A generalized Bloch equation that includes interatomic exchange effects as well as orbital motion in the gas is derived and used to interpret a recent experiment by Lewandowski *et al.* as an excitation of a collective wave of internal state polarization. It is shown that exchange leads to formation of domains in which precession frequencies are synchronized.

DOI: 10.1103/PhysRevLett.88.230403

PACS numbers: 03.75.Fi, 05.30.Jp

Atomic gases in the cold collision regime characterized by de Broglie wavelength long compared to the range of interparticle potential represent an interesting quantum many-body system. Most surprisingly, spin waves in a cold spin polarized gas are collective excitations. This phenomenon was actively studied in the 1980s, first predicted by Bashkin [1] and independently by Lhuillier and Laloë [2] and confirmed by NMR experiments in spin polarized $H \downarrow$ by Johnson *et al.* [3], in ^3He by Nacher *et al.* [4], and in dilute ^3He - ^4He mixtures by Gully and Mullin [5]. A detailed quantitative theory of the observed NMR spectra was given by Lévy and Ruckenstein [6]. Bigelow *et al.* [7] demonstrated that collective spin waves are preserved even in the Knudsen regime. The theory was further developed by Miyake *et al.* [8] and reviewed in [9].

Exchange effects in gases are not limited to spin phenomena, since any pair of internal states can play a role similar to spin states in exchange collisions [10]. Apart from new energy scales arising due to internal states spectrum, the main difference is in the anisotropic character of exchange, since for generic internal states the Hamiltonian does not have spin-rotational symmetry. Verhaar *et al.* [11] demonstrated that interatomic exchange leads to enhancement (by a factor of 2) of the density shift of Rabi transition. Similar exchange enhancement occurs in the optical spectrum density shift [12]. New aspects of cold collision exchange arise in experiments on Bose-Einstein condensation (BEC) in trapped gases. The exchange part of the density shift is absent in BEC at $T = 0$ and is reduced at $0 < T < T_{\text{BEC}}$ [12–14]. Interestingly, in this case all modes involving coupling of internal states are split into doublets [15].

In a recent experiment [16] Rabi transition was studied in a cigar shaped sample of Rb vapor contained in an Ioffe-Pritchard trap. The $|F, m_f\rangle = |1, -1\rangle, |2, 1\rangle$ levels of the hyperfine multiplet of Rb split by $\omega_0 \approx 6.8$ GHz were used. Almost perfect compensation of the density shift by spatially varying Zeeman frequency was achieved. The transition frequency varied along the sample axis by a few

tens of Hz. The initial inner state with polarization in the x - y plane was prepared by a $\frac{\pi}{2}$ pulse. It was observed that the polarization *does not remain* in the x - y plane during free Larmor precession. This was argued to result from spatial segregation of atoms with different z spin components. However, the confinement potential [16] spin dependence was very weak, and the best estimate of segregation time due to the Stern-Gerlach effect was at least an order of magnitude longer than the time ≈ 0.2 s of the z component buildup.

We argue below that the phenomena of Ref. [16] are explained by the coherent evolution of an atom's internal state rather than by mechanical segregation in the gas. The observed z component profile is readily accounted for by interatomic exchange coupling. The transition frequency [16] varies along the sample axis, and a short time after precession started a gradient of precession angle builds up. Now, consider two interacting atoms with slightly different polarization due to spatially varying Larmor frequency. The exchange interaction of these atoms leads to precession of each atom's spin around the net spin of both atoms [10]. Since both atoms have transverse polarization, the precession about a net spin (which is also transverse) will move the spins out of the x - y plane and both of them will acquire a finite z component.

Exchange effects can be illustrated by a thought experiment involving a gas of identical atoms with density n and spin $1/2$ contained in a box. Take the spin polarization \mathbf{s} to be purely transverse and the same for all atoms. For isotropic exchange coupling $\mathcal{H} = \hbar \int [\omega_0 s^z(r) + \frac{\lambda}{2} \mathbf{s}(r) \cdot \mathbf{s}(r)] d^3r$ the polarization \mathbf{s} is uniformly precessing, $\mathbf{s}(t) = \frac{1}{2}n(\cos\omega_0 t \hat{\mathbf{x}} + \sin\omega_0 t \hat{\mathbf{y}})$. Now consider a test atom passing through the box with spin polarization different from that of the other atoms. The test atom spin will experience an effective "magnetic" field $\mathbf{B} = \omega_0 \hat{\mathbf{z}} + \lambda \mathbf{s}(t)$ with the exchange part $\lambda \mathbf{s}(t)$ giving rise to Rabi transitions. In a Larmor frame rotating with frequency ω_0 about the z axis the effective field is just λn along the gas polarization \mathbf{s} , time independent in this frame. Since \mathbf{s} is

transverse, Rabi transition will generate a z component of the test atom polarization, even if initially it was in the x - y plane.

Before accepting this explanation one needs to discuss energy conservation. The probabilities to find the test atom in the up and down states after coming out of the box differ from those in the initial state, since its z spin component changes. This means that the test atom energy can change by $\hbar\omega_0$. The total energy of the system, however, does not change because the spins coupled by exchange precess together around the net spin so that the total spin is conserved [10]. The change of the net spin z component in the box is negative of the test atom spin change, as required by the energy balance.

Although this is consistent with energy conservation, the energy change of $\hbar\omega_0$ with $\omega_0 \approx 6.8$ GHz much higher than other frequencies in the system [16] may appear counterintuitive. The temperature $T = 600$ nK [16] corresponds to $k_B T / \hbar \sim 10$ KHz; the trap frequencies are $(\omega_\perp, \omega_z) = (230, 7)$ Hz. However, the characteristic exchange frequency $\lambda n \approx 140$ Hz for the typical density $n = 2 \times 10^{13} \text{ cm}^{-3}$ is much higher than the transition broadening estimated from the precession decay time to be of order of a few Hz [16]. This makes the exchange induced Rabi transitions at the energy $\hbar\omega_0$ fully coherent, despite the fact that $\hbar\omega_0 \gg \lambda n$.

The length corresponding to one Rabi cycle is

$$l_{\text{exch}} = \frac{v_T}{\lambda n} = 16 \text{ } \mu\text{m}, \quad (v_T = \sqrt{2T/m}). \quad (1)$$

This is larger than the sample radius $r_\perp = 7.3 \text{ } \mu\text{m}$ but much smaller than the sample length $r_z = 240 \text{ } \mu\text{m}$. Since movement of an atom by $\approx \frac{1}{4}l_{\text{exch}}$ is sufficient for rotat-

ing the spin by $\frac{\pi}{2}$ and moving it out of the x - y plane, the exchange coupling is a viable mechanism for spin re-orientation in this system.

The separation of Rb atoms into a gas sample and a test particle in the thought experiment is artificial. The atoms in [16] share both roles, by inducing precession on each other via exchange coupling. One therefore has to consider *collective dynamics* of atom polarization [1,2]. The Hamiltonian of Rb atoms in a trap has the form

$$\mathcal{H} = \int \left(\sum_{j=1,2} \bar{\psi}_j H_j \psi_j + \sum_{j,k=1,2} \frac{\hbar \lambda_{ij}}{2} : \hat{n}_j \hat{n}_k : \right) d^3 r, \quad (2)$$

$$H_j = -\frac{\hbar^2}{2m} \nabla^2 + U_j(r), \quad \lambda_{jk} = \frac{4\pi\hbar}{m} a_{jk}, \quad (3)$$

where $\hat{n}_j = \bar{\psi}_j \psi_j$ is the density operator. For the states used in Ref. [16] the scattering lengths are $(a_{11}, a_{22}, a_{12}) = (100.9, 95.6, 98.2)a_0$ with a_0 the Bohr's radius.

The polarization of internal states is described by "spin" operators with components given by Pauli matrices

$$\hat{s}^{x(y,z)}(r) = \frac{1}{2} \sum_{j,k} \bar{\psi}_j(r) \sigma_{jk}^{x(y,z)} \psi_k(r) \quad (4)$$

and standard spin density commutation algebra

$$[\hat{s}^\alpha(r), \hat{s}^\beta(r')] = i \varepsilon_{\alpha\beta\gamma} \hat{s}^\gamma(r) \delta(r - r'). \quad (5)$$

The system [16] is deep in the cold collision regime, since thermal de Broglie wavelength $\lambda_T = h/mv_T \approx 4000a_0$ is much larger than the scattering lengths a_{jk} . We employ the forward scattering approximation also known as the random phase approximation [17]. The interaction can be rewritten in momentum representation as

$$\int : \hat{n}_j \hat{n}_k : d^3 r = \sum_{p+p'=p''+p'''} \bar{\psi}_{j,p} \bar{\psi}_{k,p'} \psi_{j,p''} \psi_{k,p'''} = \sum_{p,p',q} (\bar{\psi}_{j,p+} \bar{\psi}_{k,p'-} \psi_{j,-p-} \psi_{k,-p'+} + \bar{\psi}_{j,p+} \bar{\psi}_{k,p'-} \psi_{j,-p'+} \psi_{k,-p-}), \quad (6)$$

where $p_\pm = p \pm q/2$. The first term of (6) accounts for the forward scattering process, while the second term describes exchange scattering. Identifying the operators in (6) with the spin density components (4) we obtain

$$: \hat{n}_1 \hat{n}_1 : = \frac{1}{2} (\hat{n} + 2\hat{s}^z)^2, \quad : \hat{n}_2 \hat{n}_2 : = \frac{1}{2} (\hat{n} - 2\hat{s}^z)^2, \quad (7)$$

$$: \hat{n}_1 \hat{n}_2 + \hat{n}_2 \hat{n}_1 : = \frac{1}{2} \hat{n}^2 - 2(\hat{s}^z)^2 + 4\hat{s}^+ \hat{s}^- + 4\hat{s}^- \hat{s}^+. \quad (8)$$

In the spin representation the interaction has the form

$$\frac{1}{2} \sum_{j,k} \lambda_{jk} : \hat{n}_j \hat{n}_k : = \frac{u}{2} \hat{n}^2 + \Lambda \hat{n} \hat{s}^z + \delta \lambda (\hat{s}^z)^2 + \lambda_{12} \mathbf{s}^2, \quad (9)$$

where $u = \lambda_{11} + \lambda_{22} + \lambda_{12}$, $\Lambda = \lambda_{11} - \lambda_{22}$, and $\delta \lambda = \lambda_{11} + \lambda_{22} - 2\lambda_{12}$. Spin dynamics is given by $\partial_t \hat{\mathbf{s}} = \frac{i}{\hbar} [\hat{\mathbf{s}}, \mathcal{H}]$, where the commutator can be evaluated with the help of the relations (5). After taking the expectation values $\mathbf{s} = \langle \hat{\mathbf{s}} \rangle$ we obtain a generalized Bloch equation

$$\partial_t \mathbf{s} + \vec{\nabla} \cdot \vec{\mathbf{j}} = \mathbf{\Omega} \times \mathbf{s}, \quad \mathbf{\Omega} = (\omega_0 + \delta \omega) \hat{\mathbf{z}} + 2\lambda_{12} \mathbf{s}, \quad (10)$$

with $\vec{\mathbf{j}}(r) = -\frac{i\hbar}{2m} \langle \bar{\psi}_j \mathbf{s}_{jk} \vec{\nabla} \psi_k \rangle + \text{H.c.}$ the spin current. Here

$$\delta \omega(r) = \frac{1}{\hbar} (U_1 - U_2) + \Lambda n + 2\delta \lambda s^z. \quad (11)$$

To make contact with the discussion in Ref. [16] we note that $\frac{1}{2} n \pm s^z = n_{1(2)}$, the occupation probabilities for the up and down spin. Combined with the form of Λ and $\delta \lambda$, the frequency $\delta \omega(r)$ can be rewritten as

$$\delta \omega(r) = \frac{1}{\hbar} (U_1 - U_2) + 2(\lambda_{11} - \lambda_{12}) n_1 - 2(\lambda_{22} - \lambda_{12}) n_2. \quad (12)$$

The first term is the Zeeman frequency shift due to the trap field inhomogeneity, while the last two terms [identical to Eq. (1) of Ref. [16]] give the density shift. The term $2\lambda_{12} \mathbf{s}$ in the expression (10) for $\mathbf{\Omega}(r)$ representing the effect of exchange is not considered in Ref. [16]. The role

of this term is subtle. It drops out from the Bloch equation (10) for \mathbf{s} , since $\mathbf{s} \times \mathbf{s} = 0$. However, since typically $2\lambda_{12}|\mathbf{s}| \gg |\delta\omega(r)|$, this term should be taken into account in the Bloch equation for other spin-related quantities, such as the spin current \mathbf{j} . The torque $\mathbf{s} \times \mathbf{j}$ (which in general is not along the z axis) makes the spin current precess so that the x , y , and z components intermix.

The transport equation for the spin current \mathbf{j} is derived in a similar fashion [1,2]. We obtain

$$\partial_t \vec{\mathbf{j}} + \alpha \vec{\nabla} \mathbf{s} = \mathbf{\Omega}(r) \times \vec{\mathbf{j}} - \gamma \vec{\mathbf{j}}, \quad \alpha = \frac{1}{3} v_T^2, \quad (13)$$

where the relaxation rate γ is added phenomenologically. The term $\alpha \vec{\nabla} \mathbf{s}$ arises in a standard way after retaining the lowest angular harmonics in the transport equation. In Eq. (13) we ignored the terms such as $\mathbf{s} \nabla(U_1 + U_2)$ and $n \hat{\mathbf{z}} \nabla(U_1 - U_2)$, since their magnitude is small (see Ref. [16]). In this approximation, the spin and density dynamics decouple, in agreement with the observation [16].

A microscopic calculation of the relaxation rate γ in Eq. (13) is nontrivial. For a spatially uniform system and spin-isotropic interaction $\gamma = 0$. Since the interaction parameters λ_{jk} for Rb coincide within 3%, spin is approximately conserved by elastic collisions. In this case, the dominant relaxation mechanism is the collisionless Landau damping [1,9,18]. We use the value $\gamma = 20$ Hz that provides the best fit to the data [16].

The transport equations (10),(13) can be simplified for a one dimensional system [16] by averaging over a sample cross section. Large exchange $\lambda n \approx \omega_{\perp}$ [16] leads to fast dynamical averaging of spin polarization in each cross section with parameters slowly varying along the sample length. In averaging Eqs. (10),(13) we assume Gaussian density profile $n(\rho) = n e^{-\rho^2/r_1^2}$. The averaging of the terms in Eqs. (10),(13) quadratic in density and/or spin is performed as $\int n^2(\rho) d^2\rho / \int n(\rho) d^2\rho = \frac{1}{2}n$, where n is the peak density. After rescaling all coupling constants

$$\lambda_{jk} \rightarrow \frac{1}{2} \lambda_{jk} \quad (14)$$

and replacing ∇ by one dimensional ∂_x we obtain transport equations of the Leggett-Rice form [19]:

$$\partial_t \mathbf{s} + \partial_x \mathbf{j} = [\omega_0 + \widetilde{\delta\omega}(x)] \hat{\mathbf{z}} \times \mathbf{s}, \quad (15)$$

$$\partial_t \mathbf{j} + a \partial_x \mathbf{s} = \{[\omega_0 + \widetilde{\delta\omega}] \hat{\mathbf{z}} + \lambda_{12} \mathbf{s}\} \times \mathbf{j} - \gamma \mathbf{j}, \quad (16)$$

$$\widetilde{\delta\omega}(x) = \frac{1}{\hbar}(U_1 - U_2) + \frac{1}{2} \Lambda n + \delta \lambda s^z. \quad (17)$$

The coupled dynamics of \mathbf{s} and \mathbf{j} is nonlinear because of the exchange precession torque $\lambda_{12} \mathbf{s} \times \mathbf{j}$ in Eq. (16).

Since $\widetilde{\delta\omega}(x), \gamma \ll \lambda_{12} n$ [16], one can simplify the equations by performing a gradient expansion. We first go to the Larmor frame rotating with frequency ω_0 , which eliminates ω_0 from Eqs. (15),(16). Next, since \mathbf{j} adiabatically follows \mathbf{s} , we ignore $\partial_t \mathbf{j}$ in Eq. (16), solve it for \mathbf{j} in terms of \mathbf{s} and $\partial_x \mathbf{s}$, and substitute the result in Eq. (15). This gives the Landau-Lifshitz equation [20]

$$[\partial_t - \partial_x D_1(\mathbf{s}) \partial_x] \mathbf{s} = [\widetilde{\delta\omega}(x) \hat{\mathbf{z}} - D_2(\mathbf{s}) \partial_x^2 \mathbf{s}] \times \mathbf{s}, \quad (18)$$

$$D_1(\mathbf{s}) = \frac{\alpha \gamma}{\gamma^2 + \lambda_{12}^2 \mathbf{s}^2}, \quad D_2(\mathbf{s}) = \frac{\alpha \lambda_{12}}{\gamma^2 + \lambda_{12}^2 \mathbf{s}^2}. \quad (19)$$

It is convenient to nondimensionalize Eq. (18). We rescale \mathbf{s} by $|\mathbf{s}|_{\max} = \frac{1}{2}n$, the frequency $\widetilde{\delta\omega}(x)$ and the relaxation rate γ by $\lambda_{12} |\mathbf{s}|_{\max}$, and choose

$$\frac{\lambda_{12} |\mathbf{s}|_{\max}}{\alpha^{1/2}} \equiv \frac{\sqrt{3}}{2} l_{\text{exch}} \approx 14 \mu\text{m} \quad (20)$$

as the length unit. Equation (18) preserves its form, with $D_2 = 1/(\gamma^2 + \mathbf{s}^2)$ and $D_1 = \gamma D_2$. The dimensionless damping is $\gamma/\lambda_{12} |\mathbf{s}|_{\max} \approx 0.31$ (see Fig. 1).

The results of the numerical simulation of Eq. (18) are shown in Fig. 1. The spatial and temporal behavior is similar to that in Ref. [16]: The z component builds up ≈ 0.2 s after precession started and then gradually decays.

Spin precession becomes *synchronized* in different parts of the sample (see Fig. 2), due to compensation of the transition frequency $\widetilde{\delta\omega}(x)$ spatial variation by the exchange field $\lambda_{12} \mathbf{s}(x)$. In our simulation, synchronization takes place independently in the domains with $s_z > 0$ and $s_z < 0$. Frequency was evaluated as

$$f = \frac{1}{2\pi} d\theta/dt, \quad \theta = \arg(s_x + i s_y). \quad (21)$$

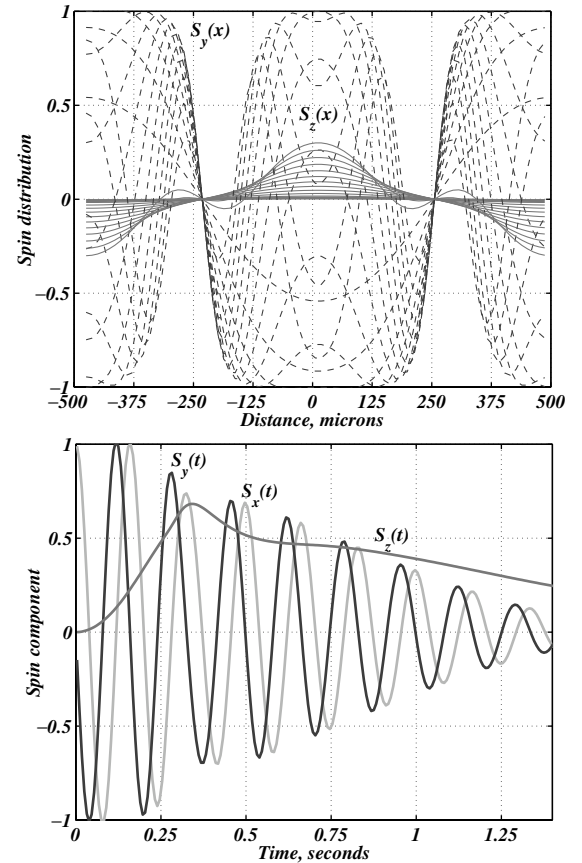


FIG. 1. Simulation of Eq. (18) with periodic boundary conditions. Parameters used: constant density $n = 2 \times 10^{13} \text{ cm}^{-3}$, exchange frequency $\lambda_{12} |\mathbf{s}|_{\max} = 70$ Hz, spatially varying frequency $\widetilde{\delta\omega}(x) = -\Omega \cos(2\pi x/L)$ with $\Omega = 20/\pi \approx 6.37$ Hz and sample size $L = 10^3 \mu\text{m}$. Top: spin distribution evolution at $0 < t < 0.2$ s; bottom: time dependence at $x = 0$.

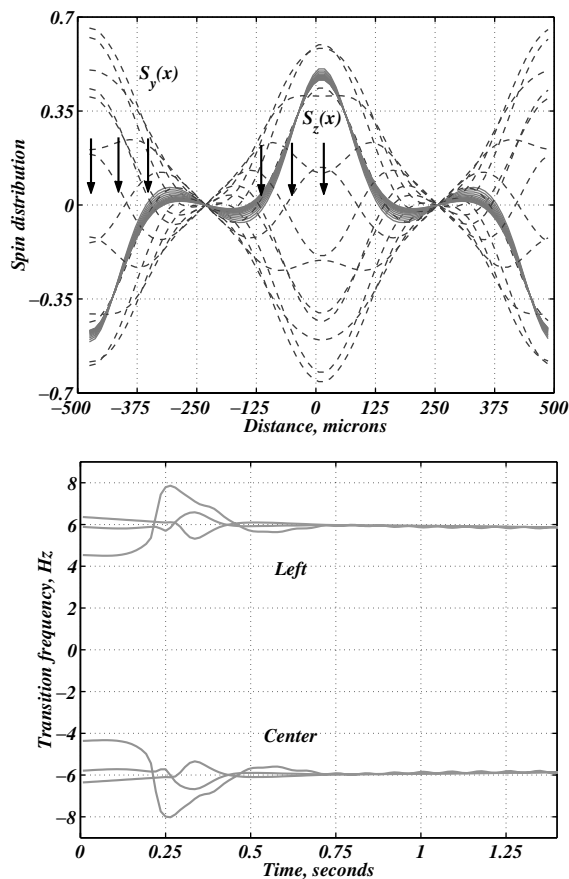


FIG. 2. Top: spin distribution evolution from 0.5 to 0.7 s (with the same parameters as in Fig. 1); bottom: frequency (21) synchronization at the points marked by arrows.

During the first 0.2 s of the z component buildup the frequency evolves from an initial value $f = \frac{1}{2\pi} \widetilde{\delta\omega}(x)$ to a constant value $\approx \pm 6$ Hz in each domain.

While precession frequencies become synchronized, the phase θ varies within each domain producing spin flux between the domains. Spin density $s(x)$ vanishes at the domain boundaries $x = \pm \frac{1}{4}L = \pm 250 \mu\text{m}$ (see Figs. 1 and 2). The number of synchronized domains and domain-specific frequency values in general depend on the amplitude and characteristic spatial scale of $\widetilde{\delta\omega}(x)$.

The mechanism of transverse spin component decay in the synchronized state is polarization mixing caused by spin current between different domains. The time scale of spin decay, set by spin diffusion, is much longer than the elastic collision time. The z component first builds up due to spin currents and then decays due to (longitudinal) diffusion, with characteristic time $(L/2\pi)^2 \gamma/\alpha \approx 0.5$ s (see Fig. 1). This is consistent with Ref. [16].

In summary, exchange coupling in a trapped gas leads to complex collective dynamics of polarization. Polarized atoms exert torque on the spin current creating a z component profile in the presence of spatially varying transition frequency, in agreement with observations [16]. Surpris-

ingly, the buildup of the z component is accompanied by synchronization of precession frequencies. In the inhomogeneous state the sample breaks into two or more synchronized domains. Spin relaxation is caused by spin currents between the domains.

Synchronized precession should manifest itself in experiment as transition frequency locking to one value in the entire sample, if it is a single domain. Several synchronized domains formed within the sample will give rise to several plateaus in the transition frequency spatial dependence. Spin density vanishing between different domains should be observable by the spatially resolved Ramsey fringes technique of Ref. [16].

We are grateful to E. A. Cornell and Tin-Lun Ho for useful discussions.

-
- [1] E. P. Bashkin, Pis'ma Zh. Eksp. Teor. Fiz. **33**, 11 (1981) [JETP Lett. **33**, 8 (1981)]; Zh. Eksp. Teor. Fiz. **87**, 1948 (1984) [Sov. Phys. JETP **60**, 1122 (1985)].
 - [2] C. Lhuillier and F. Laloë, J. Phys. (Paris) **43**, 197 (1982); **43**, 225 (1982).
 - [3] B. R. Johnson *et al.*, Phys. Rev. Lett. **52**, 1508 (1984).
 - [4] P. J. Nacher, G. Tastevin, M. Luduc, and F. Laloë, J. Phys. (Paris), Lett. **45**, L411 (1984); G. Tastevin, P. J. Nacher, M. Luduc, and F. Laloë, J. Phys. (Paris), Lett. **46**, 249 (1985).
 - [5] W. J. Gully and W. J. Mullin, Phys. Rev. Lett. **52**, 1810 (1984).
 - [6] L. P. Lévy and A. E. Ruckenstein, Phys. Rev. Lett. **52**, 1512 (1984).
 - [7] N. P. Bigelow, J. H. Freed, and D. M. Lee, Phys. Rev. Lett. **63**, 1609 (1989).
 - [8] K. Miyake, W. Mullin, and P. C. E. Stamp, J. Phys. (Paris) **46**, 663 (1985).
 - [9] E. P. Bashkin, Usp. Fiz. Nauk **148**, 433 (1986) [Sov. Phys. Usp. **29**, 238 (1986)].
 - [10] B. J. Verhaar, in *Proceedings of the 14th International Conference on Atomic Physics*, edited by D. J. Wienland, C. E. Wieman, and S. J. Smith (AIP, New York, 1995), p. 351.
 - [11] B. J. Verhaar, J. M. V. A. Koelman, H. T. C. Stoof, and O. J. Luiten, Phys. Rev. A **35**, 3825 (1987).
 - [12] M. Ö. Oktel and L. S. Levitov, Phys. Rev. Lett. **83**, 6 (1999).
 - [13] M. Ö. Oktel, T. C. Killian, D. Kleppner, and L. S. Levitov, Phys. Rev. A **65**, 033617 (2002).
 - [14] C. J. Pethick and H. T. C. Stoof, Phys. Rev. A **64**, 013618 (2001).
 - [15] M. Ö. Oktel and L. S. Levitov, cond-mat/0108052 [Phys. Rev. A (to be published)].
 - [16] H. J. Lewandowski, D. M. Harber, D. L. Whitaker, and E. A. Cornell, Phys. Rev. Lett. **88**, 070403 (2002).
 - [17] A. A. Abrikosov, L. P. Gorkov, and I. E. Dzyaloshinskii, *Methods of Quantum Field Theory in Statistical Physics* (Dover, New York, 1975), Chap. 5.
 - [18] L. S. Levitov (to be published).
 - [19] A. J. Leggett and M. J. Rice, Phys. Rev. Lett. **20**, 586 (1968).
 - [20] L. D. Landau and E. M. Lifshitz, Phys. Z. Sowjetunion **8**, 153 (1935).